

# Identifying the optimal gene and gene set in hepatocellular carcinoma based on differential expression and differential co-expression algorithm

LI-YANG DONG<sup>1\*</sup>, WEI-ZHONG ZHOU<sup>1\*</sup>, JUN-WEI NI<sup>1</sup>, WEI XIANG<sup>1</sup>,  
WEN-HAO HU<sup>1</sup>, CHANG YU<sup>1</sup> and HAI-YAN LI<sup>2</sup>

Departments of <sup>1</sup>Invasive Technology and <sup>2</sup>Rehabilitation, The First Affiliated Hospital of Wenzhou Medical University, Ou Hai, Wenzhou, Zhejiang 325000, P.R. China

Received June 23, 2016; Accepted August 10, 2016

DOI: 10.3892/or.2016.5333

**Abstract.** The objective of this study was to identify the optimal gene and gene set for hepatocellular carcinoma (HCC) utilizing differential expression and differential co-expression (DEDC) algorithm. The DEDC algorithm consisted of four parts: calculating differential expression (DE) by absolute t-value in t-statistics; computing differential co-expression (DC) based on Z-test; determining optimal thresholds on the basis of Chi-squared ( $\chi^2$ ) maximization and the corresponding gene was the optimal gene; and evaluating functional relevance of genes categorized into different partitions to determine the optimal gene set with highest mean minimum functional information (FI) gain ( $\Delta_G^*$ ). The optimal thresholds divided genes into four partitions, high DE and high DC (HDE-HDC), high DE and low DC (HDE-LDC), low DE and high DC (LDE-HDC), and low DE and low DC (LDE-LDC). In addition, the optimal gene was validated by conducting reverse transcription-polymerase chain reaction (RT-PCR) assay. The optimal threshold for DC and DE were 1.032 and 1.911, respectively. Using the optimal gene, the genes were divided into four partitions including: HDE-HDC (2,053 genes), HED-LDC (2,822 genes), LDE-HDC (2,622 genes), and LDE-LDC (6,169 genes). The optimal gene was microtubule-associated protein RP/EB family member 1 (*MAPRE1*), and RT-PCR assay validated the significant difference between the HCC and normal state. The optimal gene set was nucleoside metabolic process (GO\GO:0009116)

with  $\Delta_G^* = 18.681$  and 24 HDE-HDC partitions in total. In conclusion, we successfully investigated the optimal gene, *MAPRE1*, and gene set, nucleoside metabolic process, which may be potential biomarkers for targeted therapy and provide significant insight for revealing the pathological mechanism underlying HCC.

## Introduction

Hepatocellular carcinoma (HCC) is the fifth most common cancer worldwide and the third leading cause of cancer-related mortality (1), making it urgent to identify early diagnostic markers and therapeutic targets (2). HCC primarily develops from cirrhosis caused by chronic infection of hepatitis B virus (HBV) or hepatitis C virus (HCV), alcoholic injury, and to a lesser extent from genetically determined disorders (3). However, the heterogeneity of HCC presents unique challenges in identifying biomarkers and exploring the molecular pathogenesis in this disease (4).

With advances in high-throughput experimental technologies, they have been applied to explore diagnostic gene signatures and biological processes of human diseases (5), providing novel insights into the underlying biological mechanisms of HCC. Identifying differentially expressed genes that have similar expression profiles with known disease genes is the main method to evaluate biomarkers (6). Differential expression (DE) analysis has been widely used to explore genes with different expression levels across different conditions in many gene expression studies (7,8), especially in cancer research (9,10). Meanwhile, differential co-expression (DC) analysis mainly aims to gain insight into altered regulatory mechanisms between classes, by studying their difference in gene co-expression patterns (11). Comparing the two types of analysis, DC analysis is more suitable for identifying disease genes that may not show significant changes in expressional levels, relative to DE analysis (12,13).

From a biological perspective, if a relationship exists between DE and DC analysis, biological explanations such as cellular functions corresponding to such a dependency should be sought. The integrated DE and DC information may provide new opportunities for selecting functional relevant

---

*Correspondence to:* Dr Hai-Yan Li, Department of Rehabilitation, The First Affiliated Hospital of Wenzhou Medical University, 2 Xuexiang Road, Ou Hai, Wenzhou, Zhejiang 325000, P.R. China  
E-mail: haiyanli2016@yeah.net

\*Contributed equally

**Key words:** hepatocellular carcinoma, differential expression, differential co-expression, gene, gene set, reverse transcriptase polymerase chain reaction

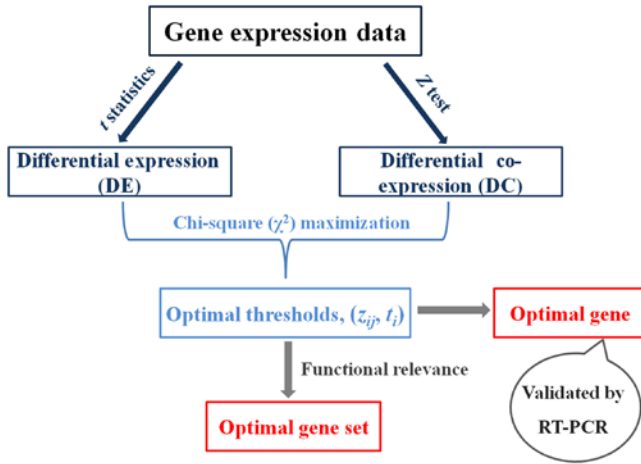


Figure 1. The scheme flow for identification of the optimal gene and gene set in hepatocellular carcinoma.

Table I. Characteristics of gene expression profiles.

Accession no.	Samples (normal/tumor)	Platform
E-GEOD-57727	62 (5/57)	A-GEOD-14951 - Illumina HumanHT-12 WG-DASL V4.0 R2 expression beadchip
E-GEOD-57957	78 (39/39)	A-GEOD-10558 - Illumina HumanHT-12 V4.0 expression beadchip

genes and dissecting complex disease mechanism. Therefore, in this study, we integrated the DE and DC together, termed the DEDC algorithm, to investigate the optimal gene and gene set for HCC. These genes and gene set may be potential biomarkers for early detection and therapeutic targets of HCC, and provide insight to reveal the underlying pathological mechanisms for this tumor.

## Materials and methods

The inference process of the optimal gene and gene set according to the DEDC algorithm was comprised of four steps: calculating DE by absolute t-value in t-statistics; computing DC based on Z-test; determining optimal thresholds dependent on Chi-squared ( $\chi^2$ ) maximization; evaluating functional relevance of genes categorized into different partitions. In addition, the optimal gene was validated by conducting reverse transcription-polymerase chain reaction (RT-PCR) assay, which further confirmed the feasibility of the DEDC algorithm. The overview of the analytical framework is illustrated in Fig. 1.

**Gene expression data.** Two gene expression profiles [E-GEOD-57727 (14) and E-GEOD-57957 (15)] for HCC were recruited from the ArrayExpress database. The characteristics are displayed in Table I. A total of 44 normal samples and 96 tumor samples were collected from the two datasets. In order to control quality of the datasets, standard pre-treatments were performed for them, which comprised

background correction based on robust multi-array average (RMA) algorithm (16); normalization performed according to quantile based algorithm (17); probe correction by Microarray Analysis Suite (MAS) software algorithm (18) and expression summarization through median polish method (16).

Subsequently, by removing invalid or duplicated probes and converting preprocessed data on the probe level into gene symbol through annotate package (19), we gained 13,666 and 13,937 genes in total in E-GEOD-57727 and E-GEOD-57957, respectively. Additionally, to remove the batch effects caused by the use of different experimentation plans and methodologies, we utilized batch mean-centering (BMC) method in inSilicoMerging package to merge the two preprocessed gene expression profiles into a single group (20). Measured gene expression values ( $x_{il}^k$ ) of gene  $i$  in sample  $l$  of the batch  $k$  were calculated by subtracting the mean  $\bar{x}_i$ :

$$\hat{x}_{il}^k = x_{il}^k - \bar{x}_i$$

**Calculating DE.** For the purpose of calculating DE levels between HCC and a normal condition, we applied absolute t-value in t-statistics to quantify the degree of DE of each gene (21). Considering the gene expression data set with  $m$  genes from samples of two conditions: one condition consisted of tumor or HCC samples ( $T$ ), while the other was composed of normal controls ( $N$ ). The absolute t-value  $|t_i|$  for a gene  $i$  ( $1 \leq i \leq m$ ) was calculated as following:

$$|t_i| = \frac{|\bar{X}_T - \bar{X}_N|}{\sqrt{\frac{V_T}{A_T} + \frac{V_N}{A_N}}}$$

Where  $\bar{X}_T$  and  $\bar{X}_N$  represent the mean expression levels in the tumor and normal conditions,  $A_T$  and  $A_N$  stand for the amount of samples in two conditions, and  $V_T$  and  $V_N$  are the standard deviations of expression levels in the tumor and normal conditions. Note that a higher absolute t-value indicates a larger DE difference.

**Computing DC.** Z-test, which quantifies the correlation difference between expression levels of two genes (12), was implemented to evaluate the DC relations between any two genes in the tumor and normal samples. For any two genes  $i$  and  $j$ , this process mainly included three steps: calculating the Pearson's correlation coefficient (PCC) separately over the samples in normal and tumor state,  $r_{ij}^N$  and  $r_{ij}^T$  (22); transforming the correlations  $r_{ij}^N$  and  $r_{ij}^T$  into normally distributed forms  $z_{ij}^N$  and  $z_{ij}^T$  by the Fisher-transforms (23); and computing the measure for DC,  $Z_{ij}$ . The calculated formulas are listed as follows:

$$r_{ij} = \frac{1}{A-1} \sum_{l=1}^A \left( \frac{g(i,l) - \bar{g}(i)}{\sigma(i)} \right) \cdot \left( \frac{g(j,l) - \bar{g}(j)}{\sigma(j)} \right)$$

Where  $A$  is the number of samples of the gene expression data;  $g(i, l)$  or  $g(j, l)$  is the expression level of gene  $i$  or  $j$  in the sample  $l$  under a specific condition;  $\bar{g}(i)$  or  $\bar{g}(j)$  represents the mean expression level of gene  $i$  or  $j$ . According to this, we could obtain  $r_{ij}^N$  for normal condition and  $r_{ij}^T$  for tumor condition. When  $r_{ij}$  indicates  $r_{ij}^N$ ,  $z_{ij}^N$  is defined as:

$$z_{ij}^N = \frac{1}{2} \ln \left| \frac{1 + r_{ij}^N}{1 - r_{ij}^N} \right|$$

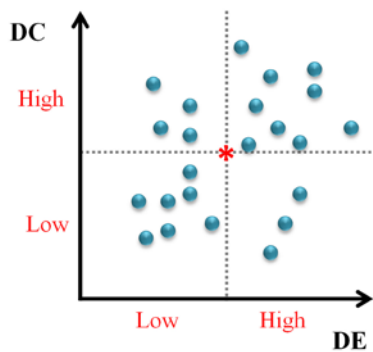


Figure 2. Genes were divided into four partitions based on the optimal differential expression (DE) and differential co-expression (DC) threshold for every gene.

$z_{ij}^T$  was evaluated similarly:

$$z_{ij}^T = \frac{1}{2} \ln \left| \frac{1 + r_{ij}^T}{1 - r_{ij}^T} \right|$$

And thus,

$$z_{ij} = \frac{|z_{ij}^N - z_{ij}^T|}{\sqrt{\frac{1}{A_N - 3} + \frac{1}{A_T - 3}}}$$

**Identifying optimal DE and DC thresholds.** With DE and DC measures defined, we investigated the relationship between DE and DC for every gene in the expression data in turn based on Pearson's  $\chi^2$  test which provided information not only on the significance of any observed differences, but also on exact categories accounting for any differences found (24). Moreover, to address whether genes with higher DC to gene  $i$  tended to (or tended not to) have higher DE, two thresholds were identified based on Pearson's  $\chi^2$  maximization, of which one was used for defining high or low DE ( $t_i$ ), and the other was employed to assess high or low DC ( $z_{ij}$ ).

**Selecting optimal threshold.** The threshold selection algorithm based on  $\chi^2$  maximization is described as follows. A pair of optimal thresholds for each gene  $i$ ,  $z_i^*$  and  $t_i^*$ , were sought from a set of threshold candidates,  $\{(z_{ij}, t_i)\}$  ( $1 \leq i, j \leq m$ ), for the DC and DE variables, respectively. To each pair of threshold candidates, every gene was categorized into one of following four partitions as shown in Fig. 2: i) low DC and low DE (LDC-LDE), termed as  $S_{LDC-LDE}$ ; ii) low DC and high DE (LDC-HDE), denoted as  $S_{LDC-HDE}$ ; iii) high DC and low DE (HDC-LDE), denoted as  $S_{HDC-LDE}$ ; and iv) high DC and high DE (HDC-HDE), denoted as  $S_{HDC-HDE}$ .

From the four partitions, we counted the number of observed genes in each partition. The observed frequency ( $O$ ) was formally defined as:  $O_{B,C} = |S_{B,C}|$  where  $B = \{LDE, HDE\}$  and  $C = \{LDC, HDC\}$ . Assuming the two DE and DC variables were independent, the expected frequency was  $E_{B,C} = \frac{O_B O_C}{m}$ . Additionally, the  $\chi^2$  value for gene  $i$  was computed as follows:

$$\chi_i^2 = \sum_{B=\{LDE, HDE\}} \sum_{C=\{LDC, HDC\}} \frac{(O_{B,C} - E_{B,C})^2}{E_{B,C}}$$

Note that there were  $m$  tests in total, since the  $\chi^2$  tests were performed for  $m$  possible threshold candidates. As a

consequence,  $m$  maximum  $\chi^2$  values were produced, and were compared with each other. We selected the threshold candidate pair with maximized  $\chi^2$  value as the pair of optimal thresholds for gene  $i$ , ( $z_i^*, t_i^*$ ).

**Performance of optimal threshold.** Some possible relationships may be presented between HDE and HDC with a certain gene, such as positive, negative and no significant relationship. To evaluate whether the association between them was significant ulteriorly, adjusted residual was employed (25), which are asymptotically standard normal results obtained from dividing it by its standard error. A cell-by-cell comparison of observed and estimated expected frequencies show the nature of the dependence. Larger values are more relevant when the degree of freedom is larger and it becomes more likely that at least one is large simply by chance (26). In this study, we defined that if the observed number of genes found in HDE and HDC partition was higher than the expected frequency, the association between HDE and HDC was regarded as positive. Conversely, if the observed frequency was less than expected, the association was considered to be negative.

**Evaluating functional relevance.** In this study, we utilized pre-defined gene sets which included Gene Ontology (GO) sets (27,28), Reactome pathways (29) and Kyoto Encyclopedia of Genes and Genomes (KEGG) pathways (30) as background data to weigh the functional relevance of the partition genes which were detected by the optimal thresholds. Firstly, to determine whether a set of partition genes was significantly overrepresented in a functional gene set or not, two-tailed Fisher's exact test based on the hyper-geometric distribution was conducted in a partition (31), and P for each gene was obtained. The P was adjusted and corrected utilizing Bonferroni (32) and Benjamini and Hochberg (33). In addition, the most significant gene set associated with the partition with the lowest P was defined as the best associated gene set.

Subsequently, functional information (FI) was proposed to perform comparison of P over different partitions (34). FI could quantify the significance of association between a gene's HDE and HDC partition  $S_{HDE-HDC}$  and a functional gene set  $G$ . When the significance of the association was high, P was small and in turn FI was high.

$$FI_{S_{HDE-HDC}G} = -\log_2(P)$$

The gain of FI by combining the HDE and HDC criteria over an individual criterion of DE for a given gene set  $G$  is defined as:

$$\Delta'_G = FI_{S_{HDE-HDC}G} - FI_{S_{HDE}G}$$

Of which  $FI_{S_{HDE}G}$  is the FI for the association between a HDE gene partition  $S_{HDE}$  and a functional gene set  $G$ . Similarly, the gain of FI,  $\Delta'_G$ , by combining the HDE and HDC criteria over an individual criterion of DC for a given gene set  $G$  was calculated. Thus, the minimum of individual FI gains could be computed as:

$$\Delta_G^* = \min(\Delta'_G, \Delta''_G)$$

The minimal FI gain was high only when both of the individual gains were high. It was low when any one of the

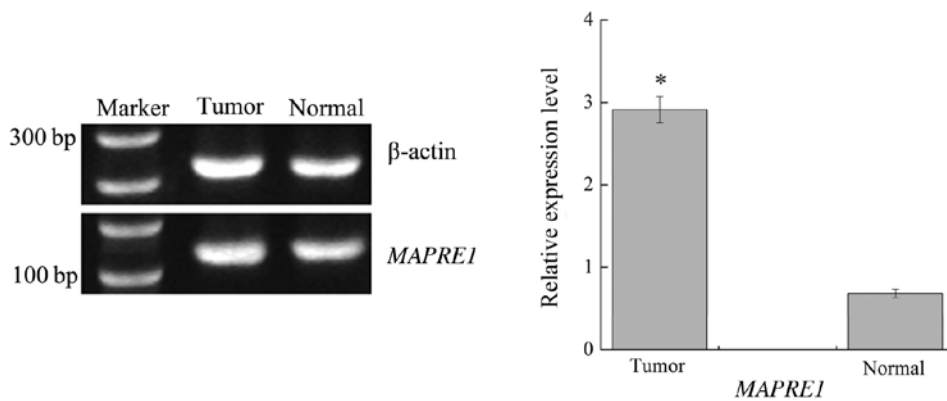


Figure 3. RT-PCR results for the optimal gene microtubule-associated protein RP/EB family member 1 (*MAPRE1*). The expression of one gene in hepatocellular carcinoma compared to normal controls was indicated by its P-value, \* $P < 0.05$ , significant change.

individual gains was low. A negative gain mean FI on the basis of the combining criteria was lower than either one or both of the individual criteria.

**Validation of the optimal gene by RT-PCR.** To validate the expression level of the optimal gene, RT-PCR assay was performed. Total RNA was prepared from HCC cell line HCC-LM3 which was kindly provided by Cancer Center, Qilu Hospital of Shandong University (Jinan, China). Cells were cultivated in Dulbecco's modified Eagle's medium (DMEM)/F-12 containing 10% fetal bovine serum (FBS) (Gibco; Life Technologies, Carlsbad, CA, USA), and antibiotics of 100 U/ml penicillin G, 100  $\mu\text{g/ml}$  streptomycin and 250 ng/ml fungizone (Carl Roth, Karlsruhe, Germany) at 37°C in a humidified incubator with 5%  $\text{CO}_2$  atmosphere (Shanghai Samsung Experimental Instrument Co., Ltd., Shanghai, China). When the cultures reached confluence (6 days), cells were treated with 0.05% trypsin/1 mM EDTA for 5 min at 37°C. Subsequently, the cell suspension was diluted with DMEM/F-12 supplemented with 10% FBS to a concentration of  $2 \times 10^5$  cells/ml, and plated in 12-well culture plates (1 ml/well). Culture medium was changed after 24 h and then every 3 days. For the cDNA synthesis, RNA was treated with Oligo (dT)<sub>18</sub> primers (Invitrogen, Carlsbad, CA, USA), 2  $\mu\text{l}$  RNasin (40 U/ $\mu\text{l}$ ), 8.0  $\mu\text{l}$  5X reverse transcriptase buffer, 8.0  $\mu\text{l}$  dNTPs and 2  $\mu\text{l}$  AMV reverse transcriptase (5 U/ $\mu\text{l}$ ). The reactions were incubated for 1 h at 42°C, 15 min at 70°C, and adjusted to a final volume of 50  $\mu\text{l}$ . The data were normalized to  $\beta$ -actin reference. The primer sequences of forward (5'-AGG CCCATCTCAACACAGAG-3') and reverse (5'-CGT TCTCTGGCAAATCAAT-3') were employed to produce an amplicon of 217 bp.

For PCR amplification, the mixture contained 10  $\mu\text{l}$  of 10X PCR buffer I and 1  $\mu\text{l}$  of *Taq* DNA polymerase (both from Invitrogen), 3  $\mu\text{l}$  of each forward and reverse primer, 8  $\mu\text{l}$  of dNTPs. Conditions were as follows: 30 sec at 95°C for pre-denaturation, followed by 35 cycles of 45 sec at 94°C, 30 sec at 55°C and 1.5 min at 72°C, and a final 10 min extension at 72°C. Three replicates of the assay within or between runs were performed to assess the reproducibility. Products of PCR experiment were analyzed by 1.5% agarose gel electrophoresis and Quantity One software of gel imaging analyzer

(Bio-Rad, Hercules, CA, USA). In addition, each test was carried out in triplicate at least and the results were analyzed using statistical process by SPSS, Inc. (Chicago, IL, USA) (35). The data are expressed as mean  $\pm$  standard deviation (SD). Differences between groups were assessed by unpaired, two-tailed Student's t-test (36).  $P < 0.05$  was considered to indicate a statistically significant difference.

## Results

**Data.** In the present study, a total of 13,666 genes were obtained in the gene expression data which included tumor (HCC) (*T*) and normal samples (*N*) for further exploitation, and thus  $m=13,666$ . When evaluating the functional relevance of the selected genes, we collected 7,114 functional gene sets or pathways in total, of which 5,895 sets were from GO, 999 sets were from Reactome pathways and 220 pathways were from KEGG pathways. To make these gene sets more reliable and confident, we took intersections between gene sets and the 13,666 genes, and selected gene sets with the number of intersected genes  $>3$  as the background gene sets. Finally, 7,103 pathways were identified for background gene sets in total.

**Optimal gene.** First of all, we calculated the DE and DC variables for the 13,666 genes in the gene expression data utilizing t-test and Z-test, respectively. Based on  $\chi^2$  maximization, the dependencies between the DE and DC variables for candidate thresholds were evaluated. We selected the maximal  $\chi^2$  value as the optimal thresholds, ( $z_i^*$ ,  $t_i^*$ ),  $z_i^*=1.032$  and  $t_i^*=1.911$ , and the corresponding gene or optimal gene was microtubule-associated protein RP/EB family member 1 (*MAPRE1*) with  $P=2.67\text{E-}43$ . The gene partitions were identified based on the optimal thresholds, which provide a flexible framework to study genes with different DE and DC characteristics (such as HDE, LDE, HDC and LDC). The significance between the DE and DC variables was calculated and the P was adjusted for multiple testing as described in the Materials and methods section. Furthermore, to evaluate whether the association between HDE and HDC was significant ultimately, adjusted residual was employed. The results showed that 2,053 genes out of all genes in the HCC data had a significant HDE and HDC association (adjusted  $P < 0.05$ ).

Table II. Top 10 best associated gene sets with highest mean minimum FI gain.

Rank	Gene sets	Gene set category	$\Delta_G^*$
1	Nucleoside metabolic process	GO\GO:0009116	18.681
2	Complement and coagulation cascades	KEGG\hsa04610	17.692
3	Nonsense mediated decay independent of the exon junction complex	REACTOME\REACT_75768.1	15.294
4	Viral gene expression	GO\GO:0019080	13.465
5	Structural constituent of ribosome	GO\GO:0003735	12.028
6	mRNA processing	GO\GO:0006397	11.794
7	Nuclear-transcribed mRNA catabolic process	GO\GO:0000956	11.389
8	Resolution of sister chromatid cohesion	REACTOME\REACT_150425.2	10.452
9	Proton-transporting two-sector ATPase complex	GO\GO:0016469	10.040
10	GTPase activity	GO\GO:0003924	9.983

FI, functional information; GO, Gene Ontology; KEGG, Kyoto Encyclopedia of Genes and Genomes.

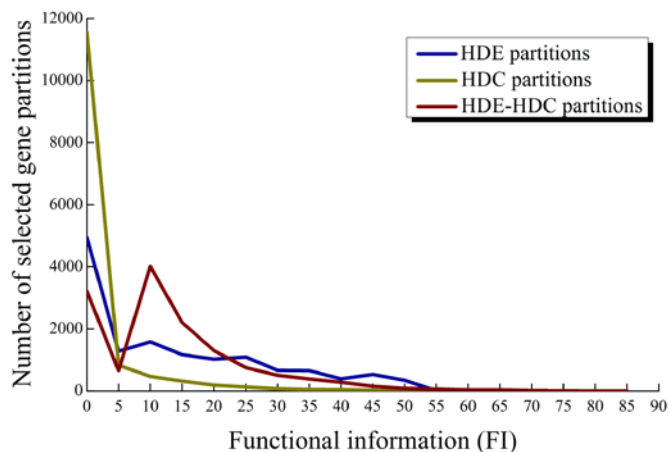


Figure 4. Distribution of functional information for high differential expression (HDE) (in blue), high differential co-expression (HDC) (in yellow) and HDE-HDC (in red) gene partitions using hepatocellular carcinoma vs. normal group.

Moreover, for the purpose of determining the expression level of the optimal gene *MAPRE1* in HCC samples and normal controls, RT-PCR analysis was conducted using the HCC cell line HCC-LM3. Three replicates were performed to make the results more reliable than for one replicate, and we took the mean value as the final outcome. The assay mainly included RNA extraction, cDNA synthesis and PCR amplification. Then the significance analysis was conducted on the results using SPSS software. The RT-PCR results are displayed in Fig. 3. We found that there was a significant difference for the relative expression level of *MAPRE1* between the HCC and normal group ( $P < 0.01$ ). Collectively, these results indicate that the gene plays an important role in the progression of HCC and confirms the feasibility of our algorithm to identify the optimal gene.

*FI of HDE-HDC partitions.* Among the HDE-HDC partitions of 2,053 genes selected from the HCC and normal set, we investigated the distribution of FI of their best associated gene sets and compared it to those using individual HDC or HDE criteria

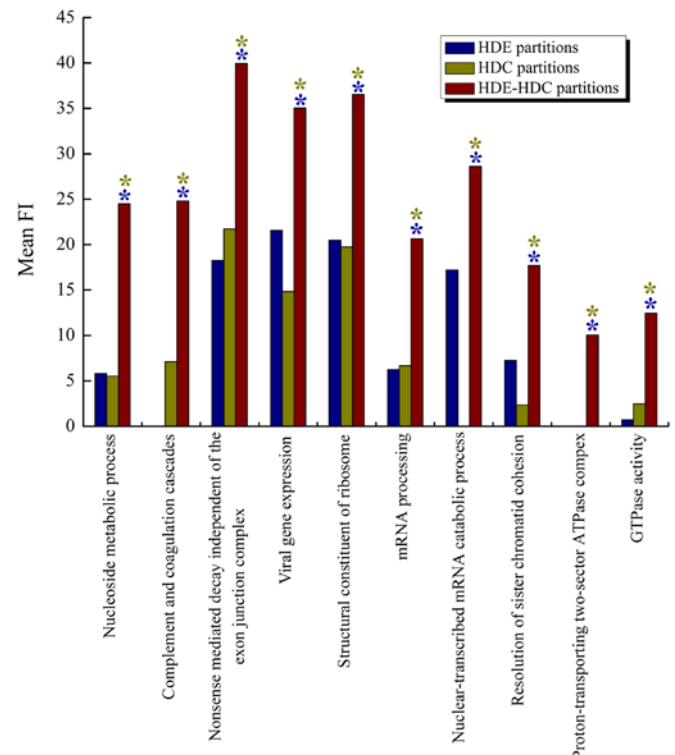


Figure 5. The top 10 best associated gene sets with high mean minimum functional information (FI) gain for high differential expression (HDE), high differential co-expression (HDC) and HDE-HDC partitions. The HDE-HDC partitions (in red) yielded significantly higher mean FI than HDE partitions (in blue) or HDC partitions (in yellow) as marked by blue or yellow asterisks, respectively. The combined HDE-HDC criteria outperformed both of the individual criteria in all gene sets (marked by blue and yellow asterisks).

based on the background gene sets and Fisher's exact test. The distributions are shown in Fig. 4. A significant observation was that when using the HDE-HDC criteria, a large group of 4,007 partitions was obtained at an FI between 5 and 10.

In addition, the best associated gene set for each gene partition of these positive associations was obtained, and the top 10 best associated gene sets with the highest mean minimum FI gain ( $\Delta_G^*$ ) are shown in Table II. The result

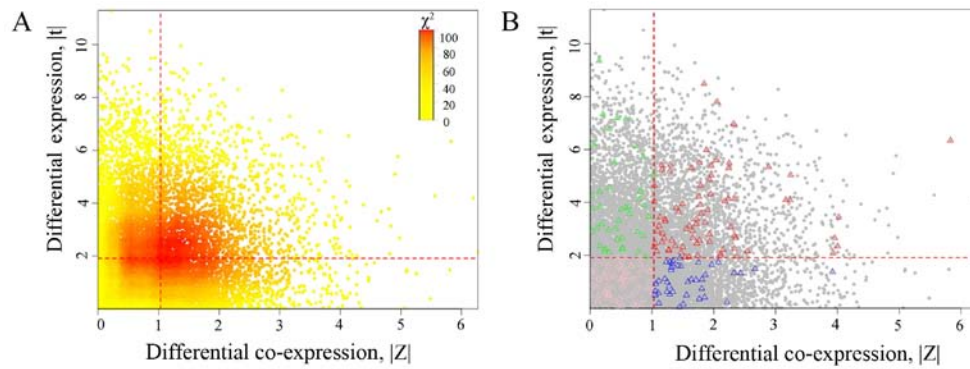


Figure 6. The scatter plot of differential expression (DE) and differential co-expression (DC) for microtubule-associated protein RP/EB family member 1 (*MAPRE1*). Each point in the plot stands for a gene. The optimal thresholds for DC and DE are indicated by red dashed lines. (A) Heatmap of the Chi-squared ( $\chi^2$ ) for the threshold candidates. (B) Gene set nucleoside metabolic process (GO\GO:0009116) was best associated with the HDE-HDC partition. The triangles represent genes found in nucleoside metabolic process and different colors denote different DE and DC values: HDE-HDC (red); LDE-HDC (blue); HDE-LDC (green); LDE-LDC (pink).

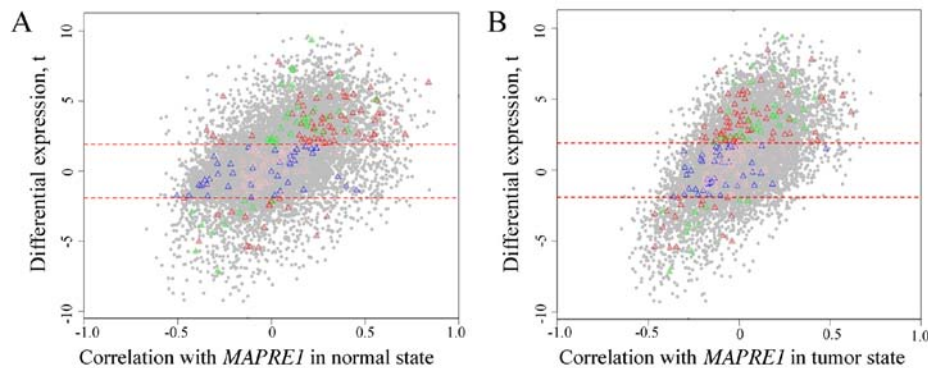


Figure 7. The scatter plot of differential expression (DE) and correlation between microtubule-associated protein RP/EB family member 1 (*MAPRE1*) and every gene in the (A) healthy state and (B) tumor state. Each point in the plot represents a gene. A positive t-value indicates a higher gene expression in the tumor state compared to the normal state, and vice versa; a negative t-value indicates a lower gene expression in the tumor state compared to the healthy state. The optimal threshold for DE is indicated using a red dashed line. The triangles represent genes found in nucleoside metabolic process, and different colors denote different DE and DC values: HDE-HDC (red); LDE-HDC (blue); HDE-LDC (green); LDE-LDC (pink).

showed that nucleoside metabolic process (GO\GO:0009116) with  $\Delta_G^*=18.681$ , complement and coagulation cascades (KEGG\hsa04610) with  $\Delta_G^*=17.692$ , and nonsense mediated decay independent of the exon junction complex (REACTOME\REACT\_75768.1) with  $\Delta_G^*=15.294$  were the top three gene sets. Fig. 5 shows the top 10 gene sets with mean FI for HDE, HDC and HDE-HDC partitions. We found that the combined HDE-HDC criteria outperformed both of the individual criteria in all gene sets, as marked by both blue and yellow asterisks.

**Association between *MAPRE1* and the nucleoside metabolic process.** To illustrate the DC and DE analysis in more detail, we selected the first ranked best association gene set for further exploration. As shown in Fig. 5, the first ranked gene set was nucleoside metabolic process. It was the best associated gene set among a total of 24 HDE-HDC partitions. Among these partitions, the gene *MAPRE1* attained a highest minimum FI gain of 18.681. Specifically, the gene set was associated with the HDE-HDC, HDE, and HDC partitions with the adjusted P of  $2.67E-43$ ,  $3.98E-07$  and  $4.24E-18$ , respectively. The average expression of *MAPRE1* in the tumor state was significantly higher than that in the normal state ( $P < 0.05$ ).

Moreover, the scatter plots of DE and DC for *MAPRE1* are shown in Fig. 6A, and red dashed lines represent the optimal thresholds. With the optimal gene of (1.032, 1.911), genes were divided into four partitions including: HDE-HDC (2,053 genes), HED-LDC (2,822 genes), LDE-HDC (2,622 genes), and LDE-LDC (6,169 genes). The amount of expected frequencies for HDE-HDC was 1667.7, which was lower than the observed 2,053, and hence the association was positive. Genes of nucleoside metabolic process in these four partitions are highlighted using triangles as shown in Fig. 6B.

The scatter plot of DE and correlation between genes and *MAPRE1* in the normal (Fig. 7A) and tumor state (Fig. 7B) are shown in Fig. 7, separately. Most selected genes in HDE-HDC partitions were more positively correlated with *MAPRE1* in the tumor group compared to the normal state. All of selected genes in the HDE-HDC partition attained a higher expression in the HCC state. There was a difference for the correlation with *MAPRE1* between the normal and tumor state. Meanwhile, a network for *MAPRE1* and 238 gene enriched in nucleoside metabolic process was constructed (Fig. 8). In the network, 79, 40, 41 and 78 genes belonged to HDE-HDC, LDE-HDC, HDE-LDC and LDE-LDC partition, respectively.

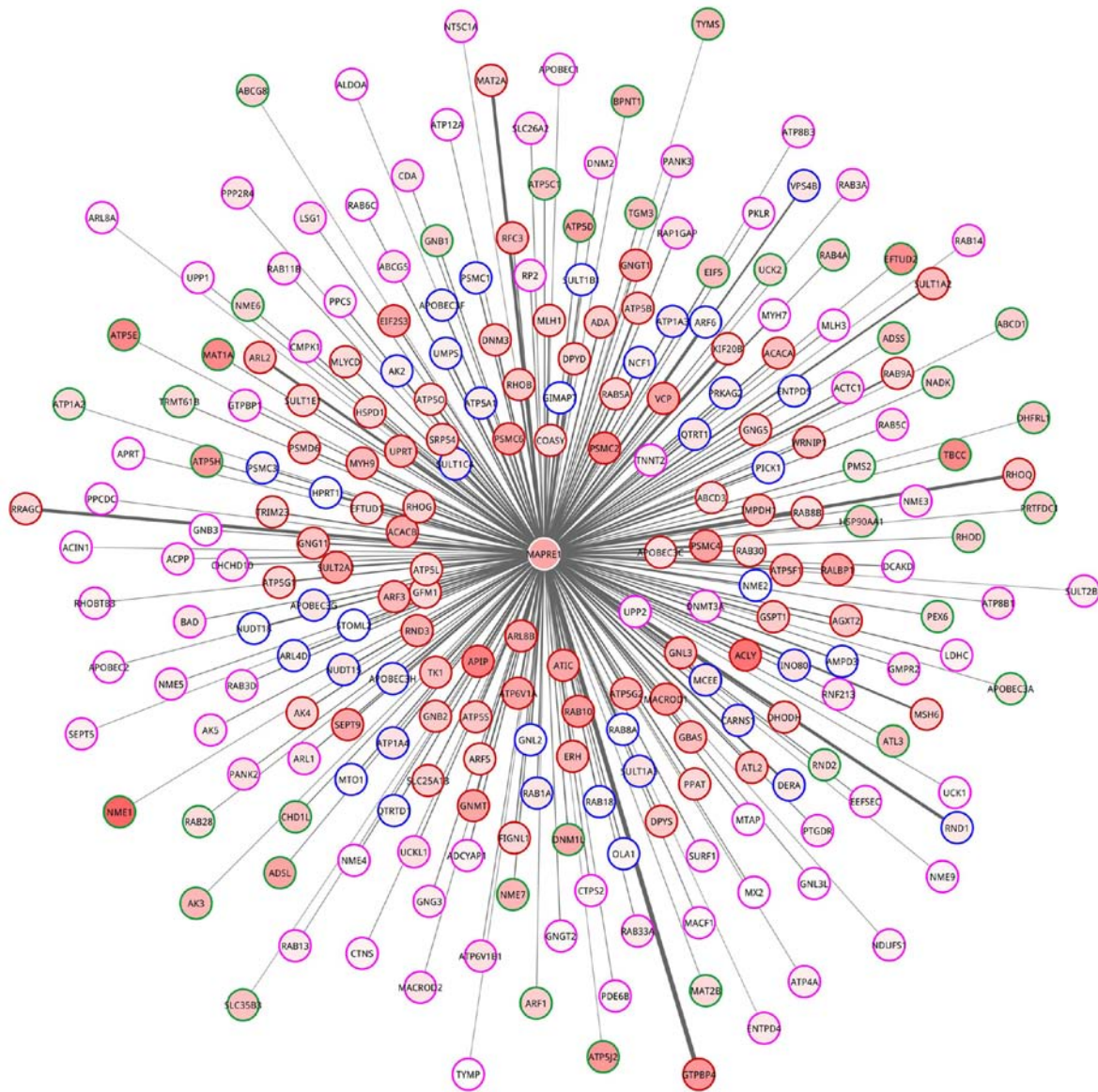


Figure 8. The network between microtubule-associated protein RP/EB family member 1 (*MAPRE1*) and nucleoside metabolic process. Nodes represent genes, and an edge stands for the interaction between two genes. Genes with higher differential expression (DE) are shaded using a deeper red color. Genes with different differential co-expression (DC) and DE values are circled with different colors: HDE-HDC (red); LDE-HDC (blue); HDE-LDC (green); LDE-LDC (pink).

## Discussion

Generally, researchers concentrate only on DE or DC analysis, and it is rarity for a study to integrate the two types of analysis together. In the present study, we employed a DEDC method which combined DE and DC analysis to investigate the optimal gene and gene set in HCC. When compared with the single approach, the DEDC algorithm is a valuable methodology for investigating biological functions of genes exhibiting disease-associated DE and DC combined characteristics, and these functional genes and processes may not be easily revealed through DE or DC approach alone. The main procedures for this approach include calculation of DE and DC levels, determination of the optimal thresholds and evaluation of functional relevance of different gene partitions. The optimal threshold for DC and DE were 1.032 and 1.911, and the corresponding gene was *MAPRE1* which was validated by

RT-PCR assay ( $P < 0.05$ ) between HCC and the normal state. This outcome also confirmed the feasibility of the DEDC method in turn.

*MAPRE1*, encoded EB1, regulates microtubule dynamic instability and chromosomal stability during mitosis, interacts with the adenomatous polyposis coli (APC) tumor suppressor, and may play an important role in tumorigenesis (37). Dysregulation of the APC-EB1 interaction, through APC mutation or EB1 overexpression, may promote cellular proliferation, spindle defects, and aberrant chromosomal segregation (38). Overexpression of *MAPRE1* has been found to induce nuclear accumulation of  $\beta$ -catenin and activate the  $\beta$ -catenin/T-cell factor pathway leading to a promotion of cell growth and increase in colony formation (39,40). Moreover, Taguchi *et al* showed a significant elevation of circulating *MAPRE1* protein in newly diagnosed and pre-diagnostic colorectal cancer plasma samples (41). It was demonstrated that

this gene was elevated in tissue from head and neck cancer (42) and was correlated with tumor size and associated with poor differentiation in HCC tissue (43). Therefore, we inferred that *MAPRE1* plays a significant role in the progression of HCC, and it was consistent with our RT-PCR result. The finding confirmed the accuracy and feasibility of the DEDC method.

Based on the DEDC algorithm, the optimal gene set was nucleoside metabolic process (GO\GO:0009116) with  $\Delta_G^* = 18.681$  and 24 HDE-HDC partitions in total. Nucleoside metabolic process refers to chemical reactions and pathways involving a nucleoside, a nucleobase linked to either  $\beta$ -D-ribofuranose (a ribonucleoside) or 2-deoxy- $\beta$ -D-ribofuranose (a deoxyribonucleoside), for example, uridine, inosine, guanosine, adenosine, cytidine and deoxyadenosine, deoxyguanosine, deoxycytidine and thymidine (44). Metabolic incorporation of azido nucleoside analogues into living cells enables sensitive detection of DNA replication through copper (I)-catalyzed azide-alkyne cycloaddition and strain-promoted azide-alkyne cycloaddition (45), whereas the altered DNA replications often lead to disease or even cancer. A previous study suggested that MYC contributes to the metabolic reprogramming of tumor cells by stimulating nucleotide synthesis and mitochondrial biogenesis (46). Recently, Laks *et al* showed that nucleoside salvage pathway kinases regulate hematopoiesis by linking nucleotide metabolism with replication stress in glioblastoma patients (47). Hence, we may deduce that nucleoside metabolic process is closely correlated to tumors. It is the first time to uncover the functions of nucleoside metabolic process in HCC.

In conclusion, we successfully investigated the optimal gene (*MAPRE1*) and gene set (nucleoside metabolic process) which may be potential biomarkers for targeted therapy and we provide significant insight for revealing the pathological mechanism underlying HCC.

## Acknowledgements

This study received no specific grants from any funding agency in public, commercial, or not-for-profit sectors.

## References

- Kaseb AO, Xiao L, Naguib R, El-Shikh W, Hassan M, Hassabo H, Lee JH, Yoon JH, Lee HS, Chae YK, *et al*: Abstract C26: Development and validation of a scoring system using insulin-like growth factor to assess hepatic reserve in hepatocellular carcinoma. *Mol Cancer Ther* 12 (Suppl 11): C26, 2013.
- Arzumanyan A, Reis HM and Feitelson MA: Pathogenic mechanisms in HBV- and HCV-associated hepatocellular carcinoma. *Nat Rev Cancer* 13: 123-135, 2013.
- Aoki T, Kokudo N, Matsuyama Y, Izumi N, Ichida T, Kudo M, Ku Y, Sakamoto M, Nakashima O, Matsui O, *et al*: Liver Cancer Study Group of Japan: Prognostic impact of spontaneous tumor rupture in patients with hepatocellular carcinoma: An analysis of 1160 cases from a nationwide survey. *Ann Surg* 259: 532-542, 2014.
- Llovet JM, Peña CE, Lathia CD, Shan M, Meinhardt G and Bruix J; SHARP Investigators Study Group: Plasma biomarkers as predictors of outcome in patients with advanced hepatocellular carcinoma. *Clin Cancer Res* 18: 2290-2300, 2012.
- Jordán F, Nguyen TP and Liu WC: Studying protein-protein interaction networks: A systems view on diseases. *Brief Funct Genomics* 11: 497-504, 2012.
- Doncheva NT, Kacprowski T and Albrecht M: Recent approaches to the prioritization of candidate disease genes. *Wiley Interdiscip Rev Syst Biol Med* 4: 429-442, 2012.
- Kulkarni H, Göring HHH, Diego V, Cole S, Walder KR, Collier GR, Blangero J and Carless MA: Association of differential gene expression with imatinib mesylate and omacetaxine mepesuccinate toxicity in lymphoblastoid cell lines. *BMC Med Genomics* 5: 37, 2012.
- McCormick KP, Willmann MR and Meyers BC: Experimental design, preprocessing, normalization and differential expression analysis of small RNA sequencing experiments. *Silence* 2: 2, 2011.
- Choi CH, Choi JJ, Park YA, Lee YY, Song SY, Sung CO, Song T, Kim MK, Kim TJ, Lee JW, *et al*: Identification of differentially expressed genes according to chemosensitivity in advanced ovarian serous adenocarcinomas: Expression of GRIA2 predicts better survival. *Br J Cancer* 107: 91-99, 2012.
- Lucas SM and Heath EI: Current challenges in development of differentially expressed and prognostic prostate cancer biomarkers. *Prostate Cancer* 2012: 640968, 2012.
- Anglani R, Creanza TM, Liuzzi VC, Piepoli A, Panza A, Andriulli A and Ancona N: Loss of connectivity in cancer co-expression networks. *PLoS One* 9: e87075-e87075, 2014.
- de la Fuente A: From 'differential expression' to 'differential networking' - identification of dysfunctional regulatory networks in diseases. *Trends Genet* 26: 326-333, 2010.
- Bockmayr M, Klauschen F, Györfy B, Denkert C and Buczies J: New network topology approaches reveal differential correlation patterns in breast cancer. *BMC Syst Biol* 7: 78, 2013.
- Cornella H, Alsinet C, Sayols S, Zhang Z, Hao K, Cabellos L, Hoshida Y, Villanueva A, Thung S, Ward SC, *et al*: Unique genomic profile of fibrolamellar hepatocellular carcinoma. *Gastroenterology* 148: 806-818, 2015.
- Mah WC, Thurnherr T, Chow PK, Chung AY, Ooi LL, Toh HC, Teh BT, Sauntharajah Y and Lee CG: Methylation profiles reveal distinct subgroup of hepatocellular carcinoma patients with poor prognosis. *PLoS One* 9: e104158, 2014.
- Irizarry RA, Bolstad BM, Collin F, Cope LM, Hobbs B and Speed TP: Summaries of Affymetrix GeneChip probe level data. *Nucleic Acids Res* 31: e15-e15, 2003.
- Bolstad BM, Irizarry RA, Astrand M and Speed TP: A comparison of normalization methods for high density oligonucleotide array data based on variance and bias. *Bioinformatics* 19: 185-193, 2003.
- Bolstad B: affy: Built-in Processing Methods, 2013. <https://www.bioconductor.org/packages/devel/bioc/vignettes/affy/inst/doc/builtinMethods.pdf>.
- Allen JD, Wang S, Chen M, Girard L, Minna JD, Xie Y and Xiao G: Probe mapping across multiple microarray platforms. *Brief Bioinform* 13: 547-554, 2012.
- Sims AH, Smethurst GJ, Hey Y, Okoniewski MJ, Pepper SD, Howell A, Miller CJ and Clarke RB: The removal of multiplicative, systematic bias allows integration of breast cancer gene expression datasets - improving meta-analysis and prediction of prognosis. *BMC Med Genomics* 1: 42, 2008.
- Asness CS, Moskowitz TJ and Pedersen LH: Value and momentum everywhere. *J Finance* 68: 929-985, 2013.
- Wang J: Pearson correlation coefficient. In: *Encyclopedia of Systems Biology*. Dubitzky W, Wolkenhauer O, Cho KH and Yokota H (eds). Springer, New York, NY, p1671, 2013.
- Gayen AK: The frequency distribution of the product-moment correlation coefficient in random samples of any size drawn from non-normal universes. *Biometrika* 38: 219-247, 1951.
- McHugh ML: The chi-square test of independence. *Biochem Med Zagreb* 23: 143-149, 2013.
- Agresti A: *Categorical Data Analysis*. 1st edition. John Wiley & Sons, New York, NY, 1996.
- Simas AB and Cordeiro GM: Adjusted Pearson residuals in exponential family nonlinear models. *J Stat Comput Simul* 79: 411-425, 2009.
- Dolinski K and Botstein D: Automating the construction of gene ontologies. *Nat Biotechnol* 31: 34-35, 2013.
- Ashburner M, Ball CA, Blake JA, Botstein D, Butler H, Cherry JM, Davis AP, Dolinski K, Dwight SS, Eppig JT, *et al*: The Gene Ontology Consortium: Gene ontology: Tool for the unification of biology. *Nat Genet* 25: 25-29, 2000.
- Croft D, O'Kelly G, Wu G, Haw R, Gillespie M, Matthews L, Caudy M, Garapati P, Gopinath K, Jassal B, *et al*: Reactome: a database of reactions, pathways and biological processes. *Nucleic Acids Res* 39: D691-D697, 2011.
- Kanehisa M, Goto S, Sato Y, Furumichi M and Tanabe M: KEGG for integration and interpretation of large-scale molecular data sets. *Nucleic Acids Res* 40: D109-D114, 2012.

31. Upton GJ: Fisher's exact test. *J R Stat Soc Ser A Stat Soc* 155: 395-402, 1992.
32. Bonferroni CE: Teoria statistica delle classi e calcolo delle probabilita. Libreria internazionale Seeber, 1936.
33. Benjamini Y and Hochberg Y: Controlling the false discovery rate: A practical and powerful approach to multiple testing. *J R Stat Soc B* 57: 289-300, 1995.
34. Lui TW, Tsui NB, Chan LW, Wong CS, Siu PM and Yung BY: DECODE: An integrated differential co-expression and differential expression analysis of gene expression data. *BMC Bioinformatics* 16: 182, 2015.
35. Bryman A and Cramer D: Quantitative Data Analysis with SPSS 12 and 13. Routledge, Hove, East Sussex, 2005.
36. Haynes W: Student's t-Test. In: Encyclopedia of Systems Biology. Dubitzky W, Wolkenhauer O, Cho KH and Yokota H (eds). Springer, New York, NY, pp2023-2025, 2013.
37. Ladd JJ, Busald T, Johnson MM, Zhang Q, Pitteri SJ, Wang H, Brenner DE, Lampe PD, Kucherlapati R, Feng Z, *et al*: Increased plasma levels of the APC-interacting protein MAPRE1, LRG1, and IGFBP2 preceding a diagnosis of colorectal cancer in women. *Cancer Prev Res (Phila)* 5: 655-664, 2012.
38. Stypula-Cyrus Y, Mutyal NN, Dela Cruz M, Kunte DP, Radosevich AJ, Wali R, Roy HK and Backman V: End-binding protein 1 (EB1) up-regulation is an early event in colorectal carcinogenesis. *FEBS Lett* 588: 829-835, 2014.
39. Liu M, Yang S, Wang Y, Zhu H, Yan S, Zhang W, Quan L, Bai J and Xu N: EB1 acts as an oncogene via activating  $\beta$ -catenin/TCF pathway to promote cellular growth and inhibit apoptosis. *Mol Carcinog* 48: 212-219, 2009.
40. Wang Y, Zhou X, Zhu H, Liu S, Zhou C, Zhang G, Xue L, Lu N, Quan L, Bai J, *et al*: Overexpression of EB1 in human esophageal squamous cell carcinoma (ESCC) may promote cellular growth by activating  $\beta$ -catenin/TCF pathway. *Oncogene* 24: 6637-6645, 2005.
41. Taguchi A, Rho JH, Yan Q, Zhang Y, Zhao Y, Xu H, Tripathi SC, Wang H, Brenner DE, Kucherlapati M, *et al*: MAPRE1 as a plasma biomarker for early-stage colorectal cancer and adenomas. *Cancer Prev Res (Phila)* 8: 1112-1119, 2015.
42. Ralhan R, Desouza LV, Matta A, Chandra Tripathi S, Ghanny S, Datta Gupta S, Bahadur S and Siu KW: Discovery and verification of head-and-neck cancer biomarkers by differential protein expression analysis using iTRAQ labeling, multidimensional liquid chromatography, and tandem mass spectrometry. *Mol Cell Proteomics* 7: 1162-1173, 2008.
43. Orimo T, Ojima H, Hiraoka N, Saito S, Kosuge T, Kakisaka T, Yokoo H, Nakanishi K, Kamiyama T, Todo S, *et al*: Proteomic profiling reveals the prognostic value of adenomatous polyposis coli-end-binding protein 1 in hepatocellular carcinoma. *Hepatology* 48: 1851-1863, 2008.
44. Waszczuk-Jankowska M, Markuszewski MJ, Markuszewski M and Kaliszan R: Comparison of RP-HPLC columns used for determination of nucleoside metabolic patterns in urine of cancer patients. *Bioanalysis* 4: 1185-1194, 2012.
45. Neef AB and Luedtke NW: An azide-modified nucleoside for metabolic labeling of DNA. *ChemBioChem* 15: 789-793, 2014.
46. Wahlström T and Henriksson MA: Impact of MYC in regulation of tumor cell metabolism. *Biochim Biophys Acta* 1849: 563-569, 2015.
47. Laks DR, Ta L, Crisman TJ, Gao F, Coppola G, Radu CG, Nathanson DA and Kornblum HI: Inhibition of nucleotide synthesis targets brain tumor stem cells in a subset of glioblastoma. *Mol Cancer Ther* 15: 1271-1278, 2016.